

4



US ARMY MEDICAL RESEARCH INSTITUTE OF CHEMICAL DEFENSE
ABERDEEN PROVING GROUND, MARYLAND 21010-5425



USAMRICD-TR-89-15

AD-A221 617

ULTRASTRUCTURAL CORRELATES OF
SULFUR MUSTARD TOXICITY

John P. Petrali
Susan B. Oglesby
Kenneth R. Mills

October 1989

DTIC
ELECTE
MAY 11 1990
S a B D

Approved for public release; distribution unlimited

US ARMY MEDICAL RESEARCH AND DEVELOPMENT COMMAND
FORT DETRICK, MARYLAND 21701-5012

90 05 11 048

UNCLASSIFIED

SECURITY CLASSIFICATION OF THIS PAGE

REPORT DOCUMENTATION PAGE

Form Approved
OMB No. 0704-0188

1a. REPORT SECURITY CLASSIFICATION UNCLASSIFIED		1b. RESTRICTIVE MARKINGS	
2a. SECURITY CLASSIFICATION AUTHORITY		3. DISTRIBUTION/AVAILABILITY OF REPORT Approved for public release; distribution is unlimited.	
2b. DECLASSIFICATION/DOWNGRADING SCHEDULE			
4. PERFORMING ORGANIZATION REPORT NUMBER(S) USAMRICD-TR-89-15		5. MONITORING ORGANIZATION REPORT NUMBER(S) USAMRICD-TR-89-15	
6a. NAME OF PERFORMING ORGANIZATION U.S. Army Medical Research Institute of Chemical Defense	6b. OFFICE SYMBOL (if applicable) SGRD-UV-YC	7a. NAME OF MONITORING ORGANIZATION U.S. Army Medical Research Institute of Chemical Defense	
6c. ADDRESS (City, State, and ZIP Code) Aberdeen Proving Ground, MD 21010-5425		7b. ADDRESS (City, State, and ZIP Code) Aberdeen Proving Ground, MD 21010-5425	
8a. NAME OF FUNDING/SPONSORING ORGANIZATION	8b. OFFICE SYMBOL (if applicable)	9. PROCUREMENT INSTRUMENT IDENTIFICATION NUMBER	
8c. ADDRESS (City, State, and ZIP Code)		10. SOURCE OF FUNDING NUMBERS	
		PROGRAM ELEMENT NO. 62787A	PROJECT NO. 3M162787A
		TASK NO. 875AA	WORK UNIT ACCESSION NO.
11. TITLE (Include Security Classification) Ultrastructural Correlates of Sulfur Mustard Toxicity			
12. PERSONAL AUTHOR(S) Petrali, J.P.; Oglesby, S.B.; and Mills, K.R.			
13a. TYPE OF REPORT Final	13b. TIME COVERED FROM Feb1986 TO Jun1989	14. DATE OF REPORT (Year, Month, Day) October 1989	15. PAGE COUNT 31
16. SUPPLEMENTARY NOTATION			
17. COSATI CODES		18. SUBJECT TERMS (Continue on reverse if necessary and identify by block number)	
FIELD 06	GROUP 11	→ Sulfur mustard (HD), toxicity, lymphocytes in vitro, keratinocytes in culture, skin, ultrastructure, pathology.	
19. ABSTRACT (Continue on reverse if necessary and identify by block number) Standardized ultrastructural technology was used to study subcellular effects of sulfur mustard (HD) on 1) human lymphocytes <u>in vitro</u> , 2) human keratinocytes in culture, and 3) the skin of the hairless guinea pig. While doses of mustard differed according to the dictates of individual protocols, all specimens were gathered 24 hours following exposure, aldehyde fixed, and processed for transmission and scanning electron microscopy. In the hairless guinea pig model the subcellular effects on basal cells of the stratum germinativum and the generation of microblisters at the dermal-epidermal junction were unequivocal to that reported for human-skin grafted to congenitally athymic nude mice. Basal cell degenerative changes, signalled by nuclear condensations, blebbing of the nuclear envelope, and defects of the plasmalemma, progressed to paranuclear cytoplasmic vacuolations, loss of cellular organelles, lipid inclusions, increased lysosomal activity, and necrosis. Boundaries of the microblister, components of the roof and floor of the blister cavity, and			
20. DISTRIBUTION/AVAILABILITY OF ABSTRACT <input checked="" type="checkbox"/> UNCLASSIFIED/UNLIMITED <input type="checkbox"/> SAME AS RPT. <input type="checkbox"/> DTIC USERS		21. ABSTRACT SECURITY CLASSIFICATION UNCLASSIFIED	
22a. NAME OF RESPONSIBLE INDIVIDUAL DAVID H. MOORE, MAJ, VC, C, Pathophysiology Div		22b. TELEPHONE (Include Area Code) (301) 671-2553	22c. OFFICE SYMBOL SGRD-UV-Y

DD Form 1473, JUN 86

Previous editions are obsolete.

SECURITY CLASSIFICATION OF THIS PAGE
UNCLASSIFIED

19. Continued

apparent disabling of anchoring filaments of hemidesmosomes in the formation of the microblister were also similar. In human lymphocytes in vitro and human keratinocytes in culture, HD-induced pathology was identical to that of the basal cell of the skin models. Nuclear chromatin condensations, nuclear envelope blebbing and interruptions of the plasmalemma were again persistent temporal ultrastructural features of the cascading cellular pathology of HD-induced toxicity. It is expected that establishing and comparing ultrastructural correlates of HD toxicity in differing model systems will provide a useful morphological database against which prophylactic and therapeutic regimens might be measured.

PREFACE

This ultrastructural study on the comparison of effects of HD-induced toxicity in differing model systems was performed under task area 875, research plan # 1-01-1-06-0000, protocols # 1-20-88-000-B-497 and 1-01-83-000-B-220, and satisfied JSA requirements STO-01,02,03. All ultrastructural protocols and experimental data were recorded in laboratory notebook #16-86 assigned to Dr. Petrali.

Accession For	
NTIS GRA&I	<input checked="" type="checkbox"/>
DTIC TAB	<input type="checkbox"/>
Unannounced	<input type="checkbox"/>
Justification	
By _____	
Distribution/	
Availability Codes	
Dist	Avail and/or Special
A-1	

FIGURES

	Page No.
1. Semithin Epoxy Sections of the Dermal-epidermal Junction of Hairless Guinea Pig Skin	4
2. Scanning Electron Microscopy of the Dermal-epidermal Junction of Hairless Guinea Pig Skin	5
3. Transmission Electron Microscopy of Hairless Guinea Pig Skin	6
4. Semithin Sections of Epoxy Embedded Human Lymphocytes	11
5. Semithin Epoxy Sections of Human Keratinocytes	12
6. Scanning Electron Microscopy of Human Lymphocytes	13
7. Scanning Electron Microscopy of Human Keratinocytes	14
8. Transmission Electron Microscopy of Human Lymphocytes	15
9. Transmission Electron Microscopy of Human Keratinocytes.	19

INTRODUCTION

Despite 60 years of intensive research on mechanisms of sulfur mustard (HD) injury, the ultrastructural pathology of HD-induced toxicity has only recently been investigated. The first subcellular study was published in our report on the ultrastructure of the pathogenesis of blister formation following exposure to sulfur mustard of human-skin grafted to congenitally athymic nude mice.¹ This ultrastructural analysis allowed us to effect several objectives: 1) to further delineate the histopathology which had been noted earlier at light microscopy levels, 2) to identify possible mustard-induced morphological changes which may occur during the latent asymptomatic phase, and 3) to promote our understanding of the temporal features of mustard pathology with the expectation that prophylactic and therapeutic strategies might be morphologically predictable. Now, we are able to describe and compare the fine structural pathology of HD-induced toxicity of human lymphocytes *in vitro*,^{2,3} human keratinocytes in culture and a hairless guinea pig model,⁴ and to correlate these ultrastructural pathologies with those associated with the HD-induced lesion already reported for the human-skin grafted to congenitally athymic nude mouse model.

MATERIALS AND METHODS

We used standardized ultrastructural technology to study by transmission and scanning electron microscopy the subcellular effects of HD in human lymphocytes *in vitro*, human keratinocytes in culture, and the hairless guinea pig. While doses of mustard differed according to the dictates of individual protocols (human lymphocytes, 1×10^{-3} molar HD for 24 hours; human keratinocytes 6×10^{-4} molar HD for 24 hours; hairless guinea pig, 2.0 μ l HD for 30 minutes), all specimens were gathered 24 hours following exposure and were processed as follows. Control and HD-exposed human lymphocytes and human keratinocytes were rinsed in their respective suspension media followed then by three 10-minute washes in 0.1M sodium cacodylate, at pH 7.34, 190 mOsm, and centrifuged for 10 minutes at 250xG at 20°C. The resulting cell pellet was fixed for one hour in cacodylate-buffered combined aldehyde fixative of 1.6% formaldehyde and 2.5% glutaraldehyde. Selected skin samples of the hairless guinea pig were fixed in buffered 4% formaldehyde and 1% glutaraldehyde for 48 hours. Cells and skin samples were post fixed in buffered 1% osmium tetroxide for one hour, dehydrated in graded ethanols and embedded in epoxy resin. Semithin sections, 1 micron thick, were differentiated with Humphrey's stain,⁵ and observed by light microscopy. Ultrathin sections, 100nm thick, were counterstained with uranyl acetate and lead citrate for analysis by transmission electron microscopy (JEOL, 1200EX). Remaining samples, not embedded, were critical-point dried, sputter coated with gold palladium and examined by scanning electron microscopy (AMRAY, 1200B).

RESULTS

In the hairless guinea pig model the cellular and subcellular effects on basal cells of the stratum germinativum and the generation of the microblister at the dermal-epidermal junction were the same as that reported for the human-skin grafted model (Fig. 1). Boundaries of the microblister, components of the roof and floor of the blister cavity, and the apparent disabling of anchoring filaments of hemidesmosomes in the formation of the microblister were also similar (Fig. 2). Skin basal cell degenerative changes, signalled by nuclear condensations, blebbing of the nuclear envelope and defects of the plasmalemma at the perimeter of the microblister progressed to paranuclear cytoplasmic vacuolations, loss of cellular organelles, lipid inclusions, increased lysosomal activity, and complete cellular necrosis at the center of the microblister (Fig. 3).

In the case of human lymphocytes and human keratinocytes the HD-induced pathology was identical to that of the basal cell of the skin model (Figs. 4,5). An obvious feature of isolated cell toxicity was loss of microvilli and disruptions of the plasmalemma. These were especially evident upon scanning microscopic study (Figs. 6,7). Nuclear chromatin condensations, blebbing of the nuclear envelope, interruptions of the plasmalemma, progressive cytoplasmic vacuolation, loss of cellular organelles, increased lysosomal activity and necrosis were, again, persistent and successive ultrastructural features of the cascading cellular pathology of HD-induced toxicity (Figs. 8,9).

DISCUSSION AND CONCLUSIONS

The results of this study would suggest that the ultrastructural temporal features of HD-induced toxicity are similar and persistent within the human-skin graft model, the hairless guinea pig model, human lymphocytes *in vitro*, and human keratinocytes in culture. In the skin studies, development of apparent initial nuclear pathology of basal cells of the stratum germinativum was followed by progressive cytoplasmic changes leading to eventual death of affected cells. Interruptions of the anchoring filaments of basal cell hemidesmosomes at the dermal-epidermal junction were a persistent feature of the pathogenesis of microblister formation. In the case of the human lymphocyte and human keratinocyte, although sequential events could not be established in this single time study, the apparent developing ultrastructural pathology, beginning with nuclear changes and subsequent cytoplasmic alterations appears identical to that of the basal cell.

It is not possible to conclude whether the ultrastructural changes observed in this study are specific for HD. Basal cell responses to other toxins, such as proteases and endogenous toxins⁶⁷ indicate that the basal cell may respond

stereotypically to a variety of insults. Although this non-specific response may secondarily initiate the loss of integrity of anchoring filaments of the dermal-epidermal junction, it has been suggested that a protease, specific for anchoring filaments, may be released as a result of the biochemical changes associated with skin-mustard toxicity.¹ In any event, it points to the vulnerability of the basal cell, as well as the dermal-epidermal junction of the skin as a site of primary lesion in skin pathologies.

Responses of the isolated human lymphocyte and human keratinocyte to similar toxins have not been firmly established. However, this present study would indicate that the response of these isolated cells to HD and other toxins would be expected to be similar to that of the basal cell.

Additional model systems useful for HD-toxicity study should be subjected to similar ultrastructural investigations with the anticipation that persistent subcellular features of HD-induced toxicity may prove useful in predicting and measuring prophylactic and therapeutic strategies.

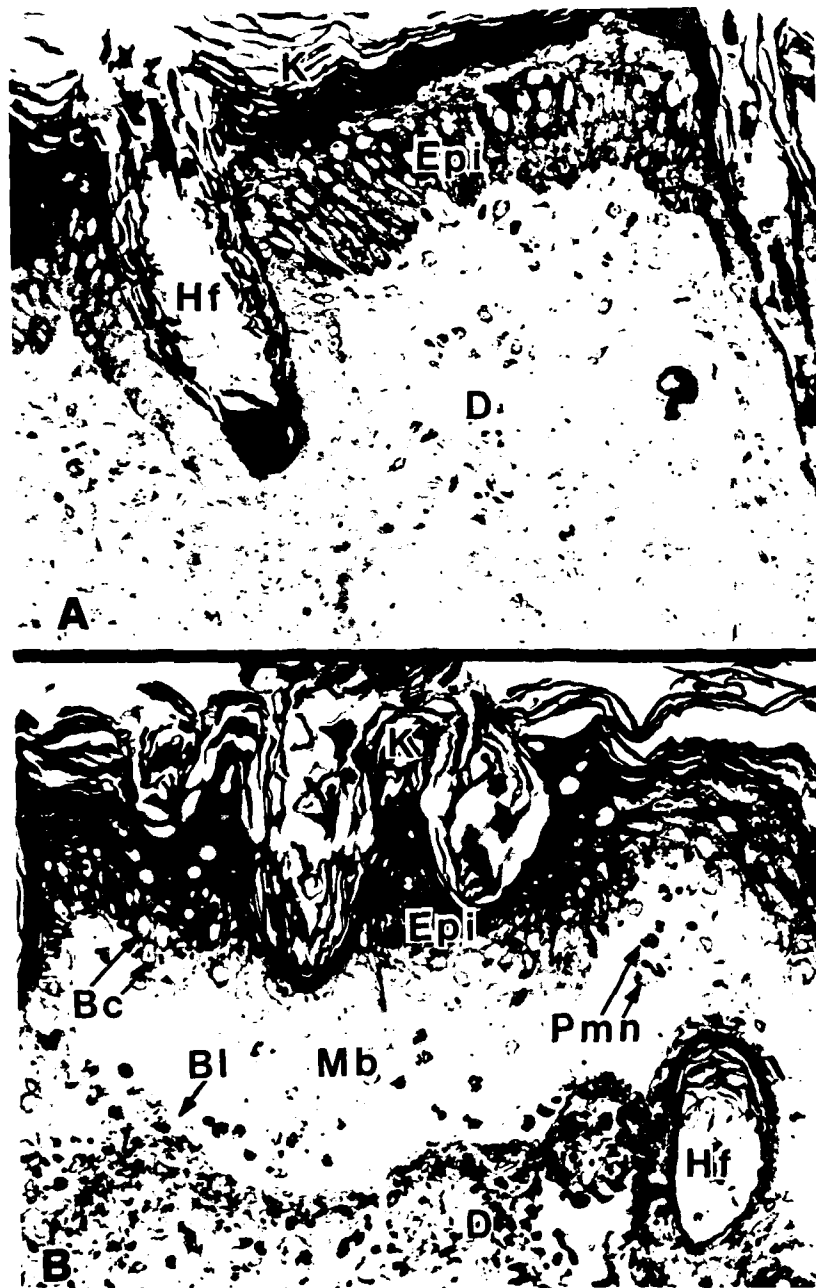


Figure 1. Semithin epoxy sections of the dermal-epidermal junction of hairless guinea pig skin. A. Non-blistered skin; epidermis (Epi), dermis (D), keratin (K), hair follicle (Hf). B. Microblister (Mb) cavity infiltrated with polymorphonuclear leukocytes (Pmn) and cellular debris. The basal lamina (Bl) forms the floor of the cavity with the roof formed by basal cells (Bc) of the epidermis. 330X.

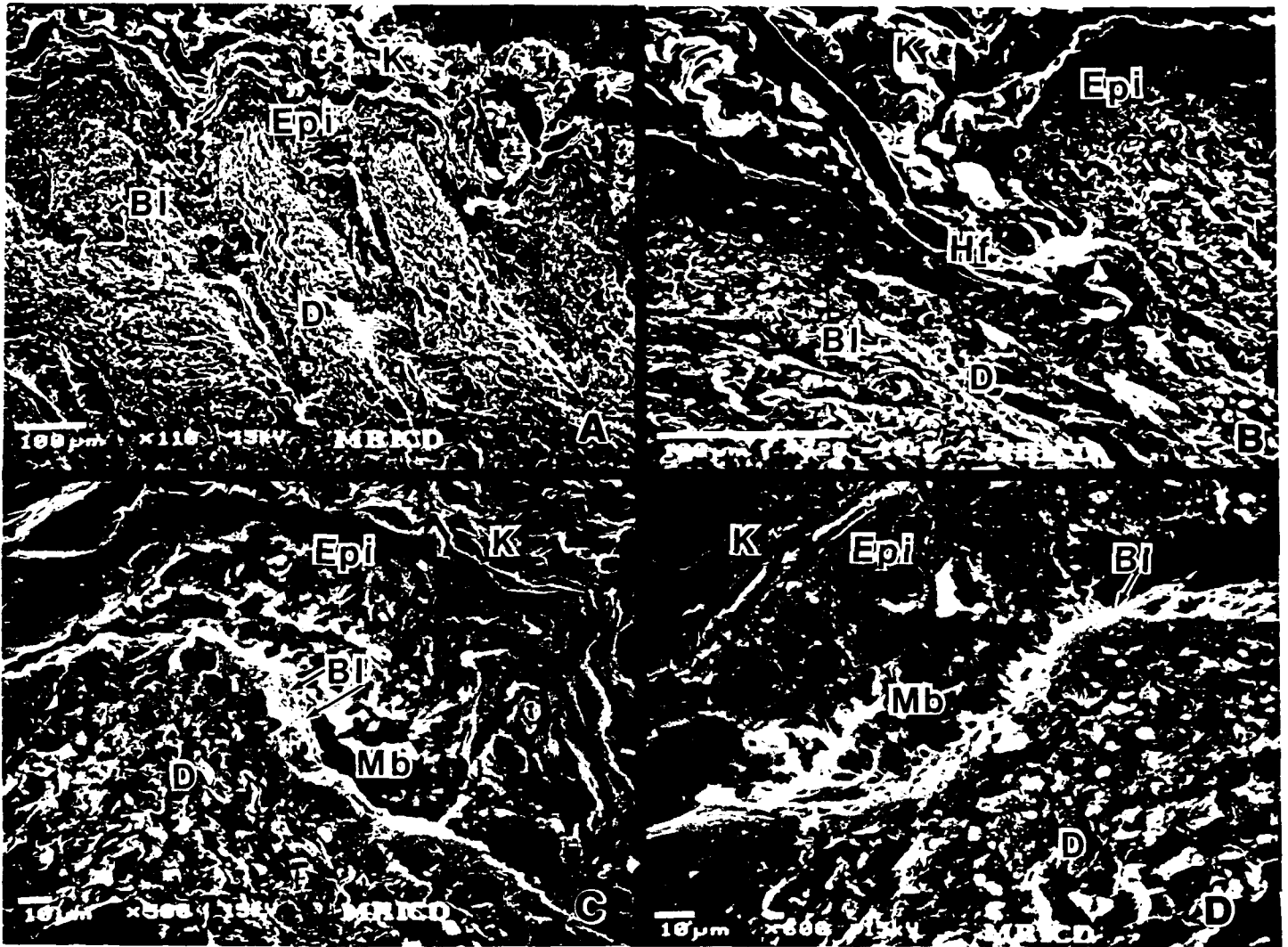
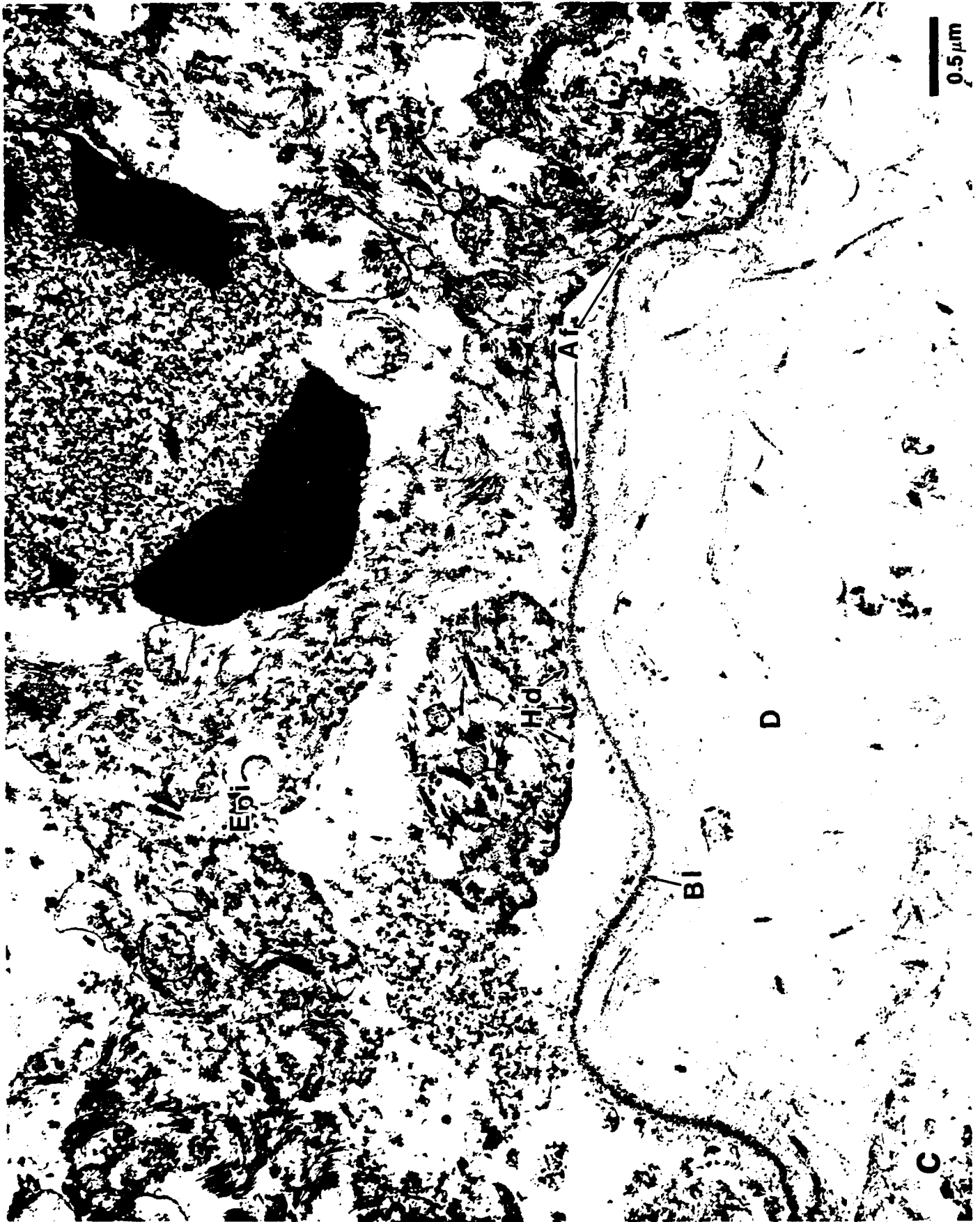


Figure 2. Scanning electron microscopy of the dermal-epidermal junction of hairless guinea pig skin. A,B. Non-blistered skin; epidermis (Epi), dermis (D), keratin (K), hair follicle (Hf), basal lamina (Bl). C,D. Microblistered skin. Microblister cavity (Mb) is bordered by cells of the epidermis at the roof and the basal lamina at the floor.

Figure 3. Transmission electron microscopy of hairless guinea pig skin. A. Dermal-epidermal junction of intact non-exposed skin. Basal cell (Bc), basal lamina (Bl), hemidesmosomes (Hd), nucleus of basal cell (N), dermis (D), lamina lucida (Ll), epidermis (Epi). B,C. Dermal-epidermal junction at the periphery of a microblister of HD-exposed skin demonstrating effects on basal cells and the disabling of anchoring filaments at the lamina lucida. Perinuclear bleb (Pb), nuclear condensation (Nc), cytoplasmic vacuoles (V), anchoring filaments (Af), hemidesmosomes (Hd). D. Center of the microblister cavity showing invading neutrophils (Ne) and cellular debris (arrows).









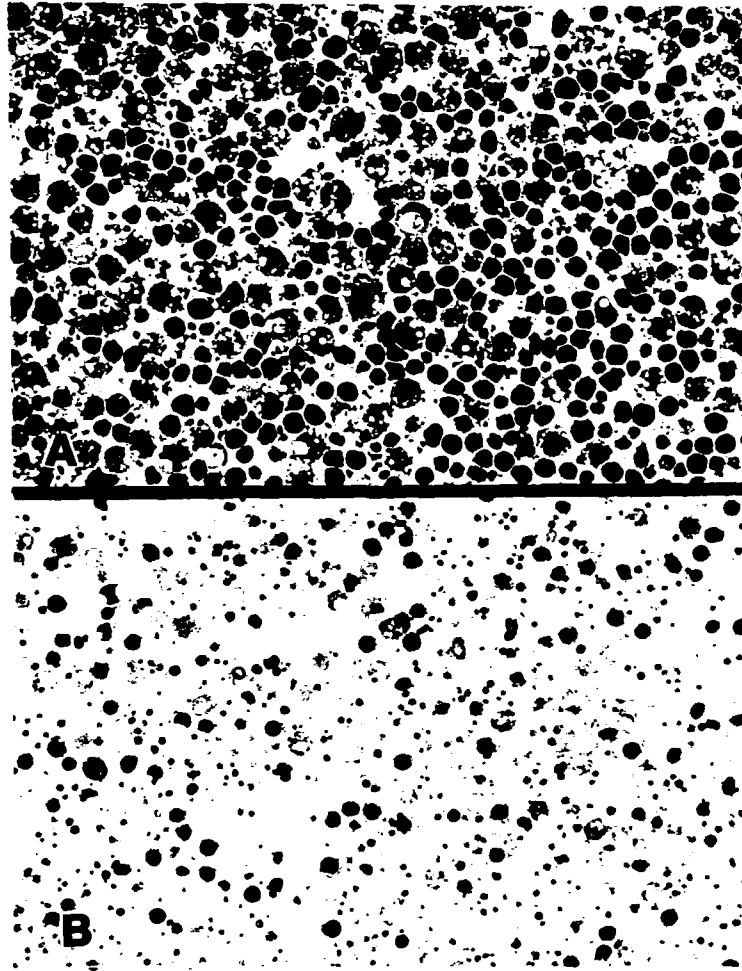


Figure 4. Semithin sections of epoxy embedded human lymphocytes. A. Control sample. Viability as determined by dye exclusion was 84%. B. HD-exposed lymphocytes. Ultrastructural changes include condensation of nuclear chromatin, paranuclear vacuolation and necrosis. Viability of this sample was 30%.

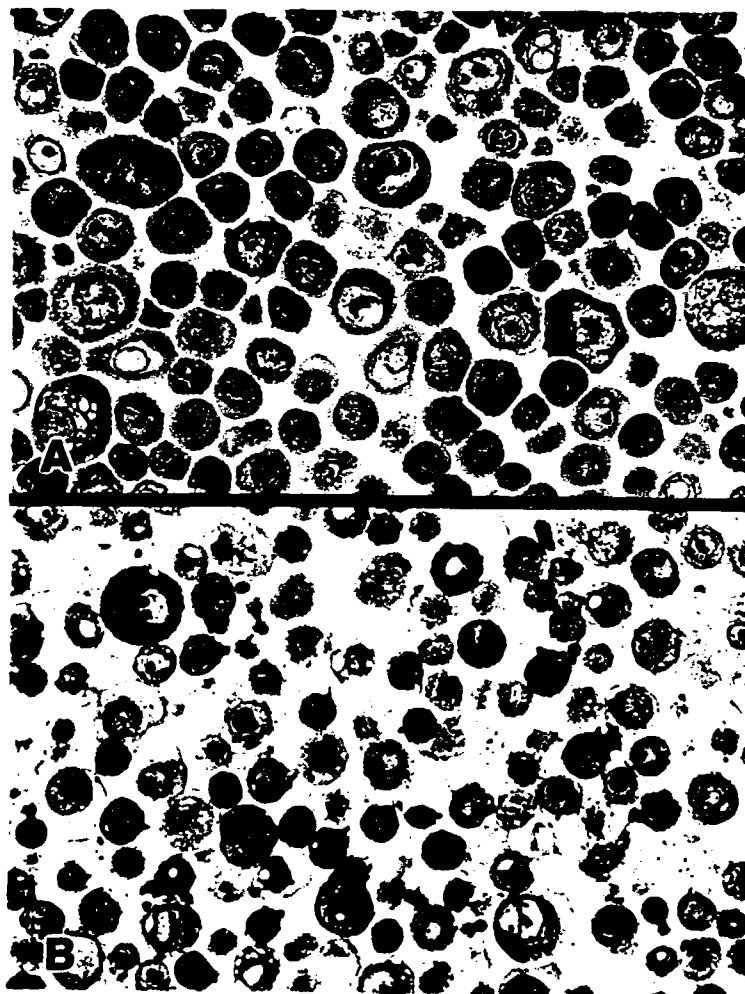


Figure 5. Semithin epoxy sections of human keratinocytes. A. Control sample. Cells are mitotically active and demonstrate a viability of 87%. B. HD-exposed human keratinocytes show typical HD-induced changes as described for lymphocytes. Viability of this group was 47%.

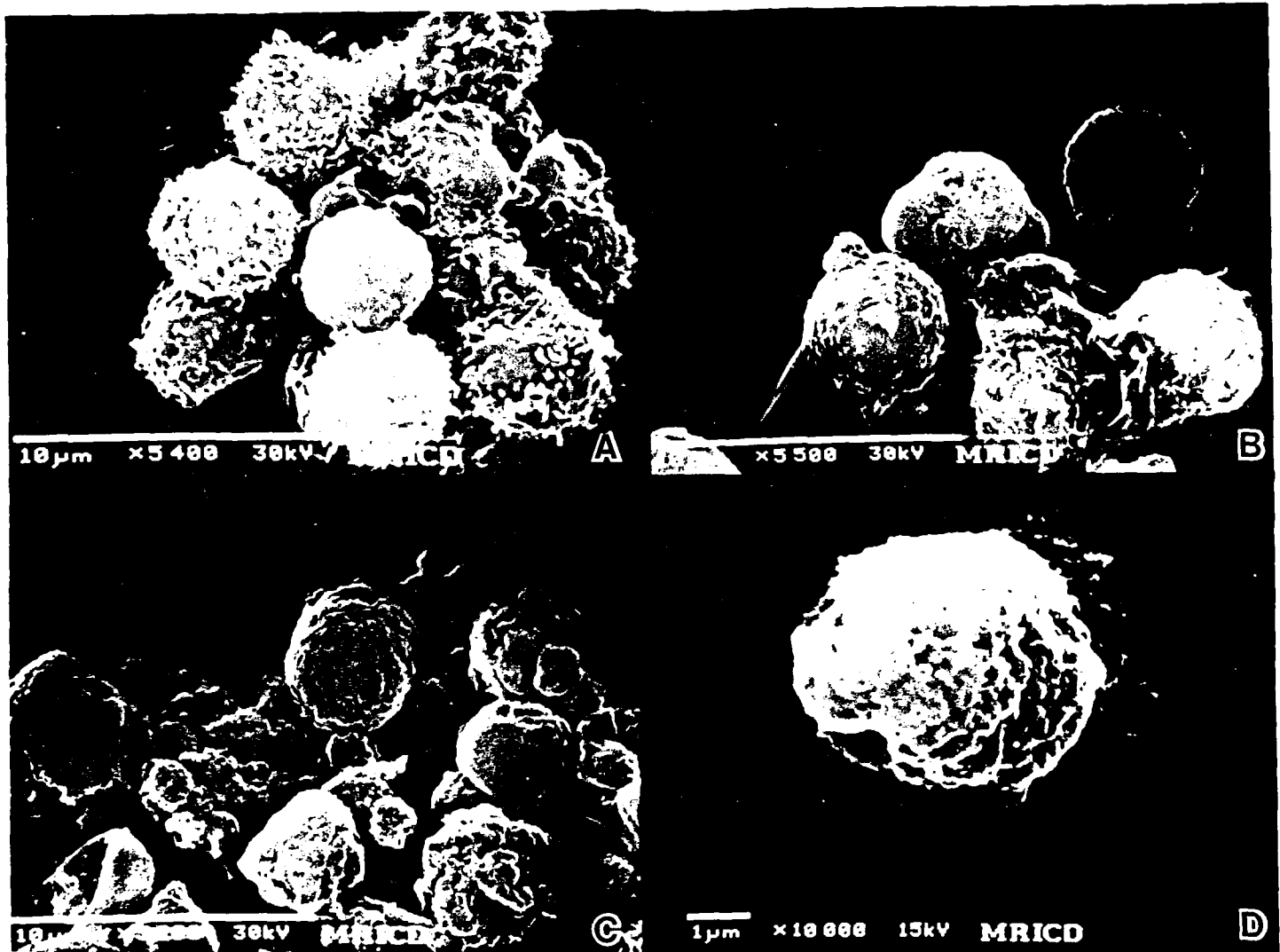


Figure 6. Scanning electron microscopy of human lymphocytes. A. Control lymphocytes showing typical surface features, including abundant microvilli and uninterrupted plasma membrane. B,C. HD-exposed lymphocytes have lost microvilli, are fragmented and present many perforations of the plasma membrane. D. Higher magnification of an isolated cell showing perforations of the plasma membrane.

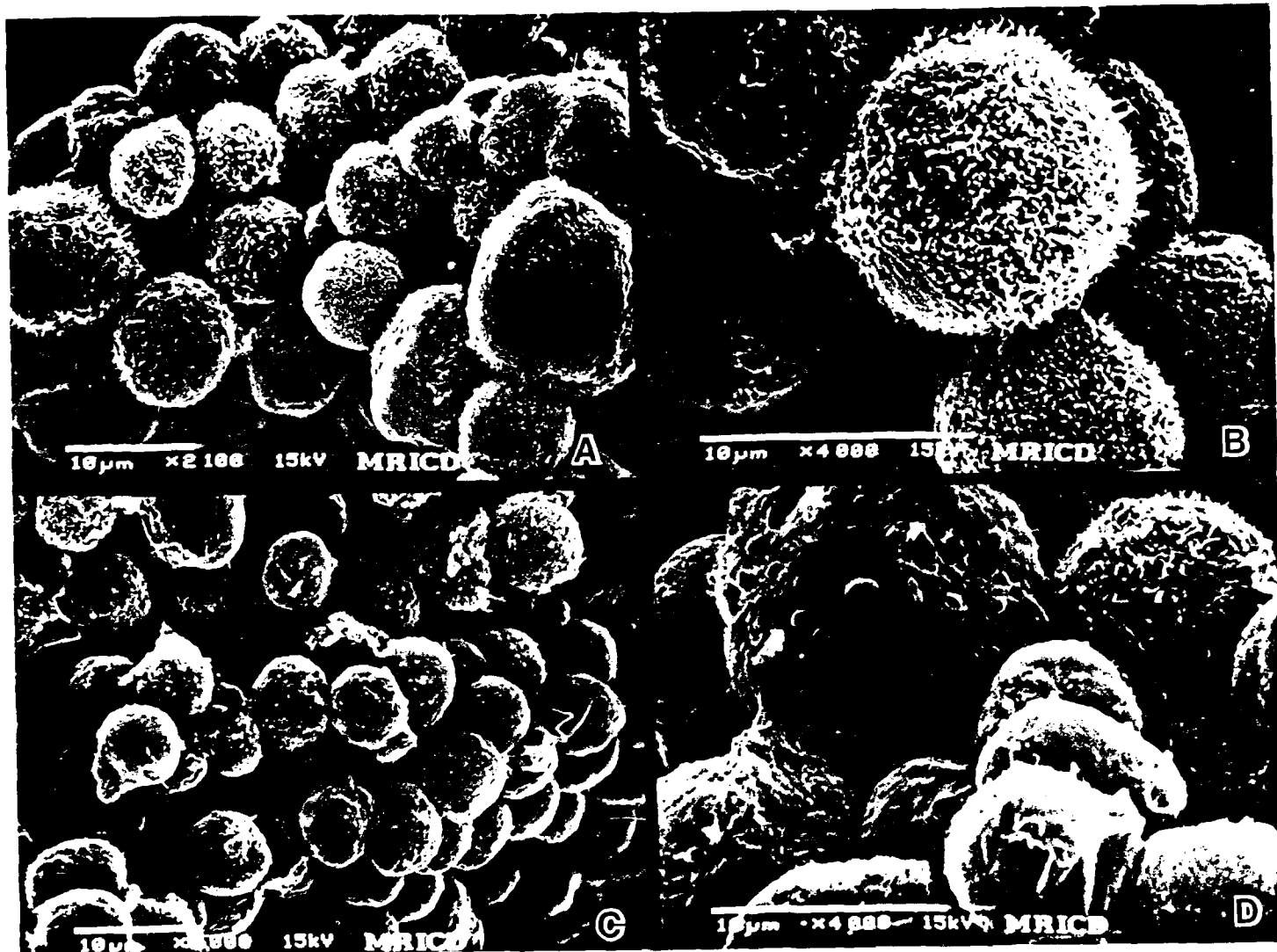


Figure 7. Scanning electron microscopy of human keratinocytes. A,B. Control keratinocytes showing typical surface features, including abundant microvilli and uninterrupted plasma membrane. C. Survey picture of keratinocytes exposed to HD. Cells have lost microvilli, and demonstrate blebbing and irregularities of the plasma membrane. D. Higher magnification of HD-exposed keratinocytes showing to advantage blebbing and perforations of the plasma membrane and loss of microvilli.

Figure 8. Transmission electron microscopy of human lymphocytes. A. Representative cell of the control group showing typical fine structural features of a medium-sized lymphocyte; nucleus (N), nuclear membrane (Nm), mitochondria (M), plasma membrane (Pm), ribosomes (R), microvilli (Mv). B,C. Lymphocytes exposed to HD displaying subcellular changes including condensation of nuclear chromatin, blebbing of the nuclear membrane (Pb), progressive cytoplasmic vacuolations (V), increased lysosomal activity (Ly), blebbing of the plasma membrane (Cb), and perforations of the plasmalemma (arrows).

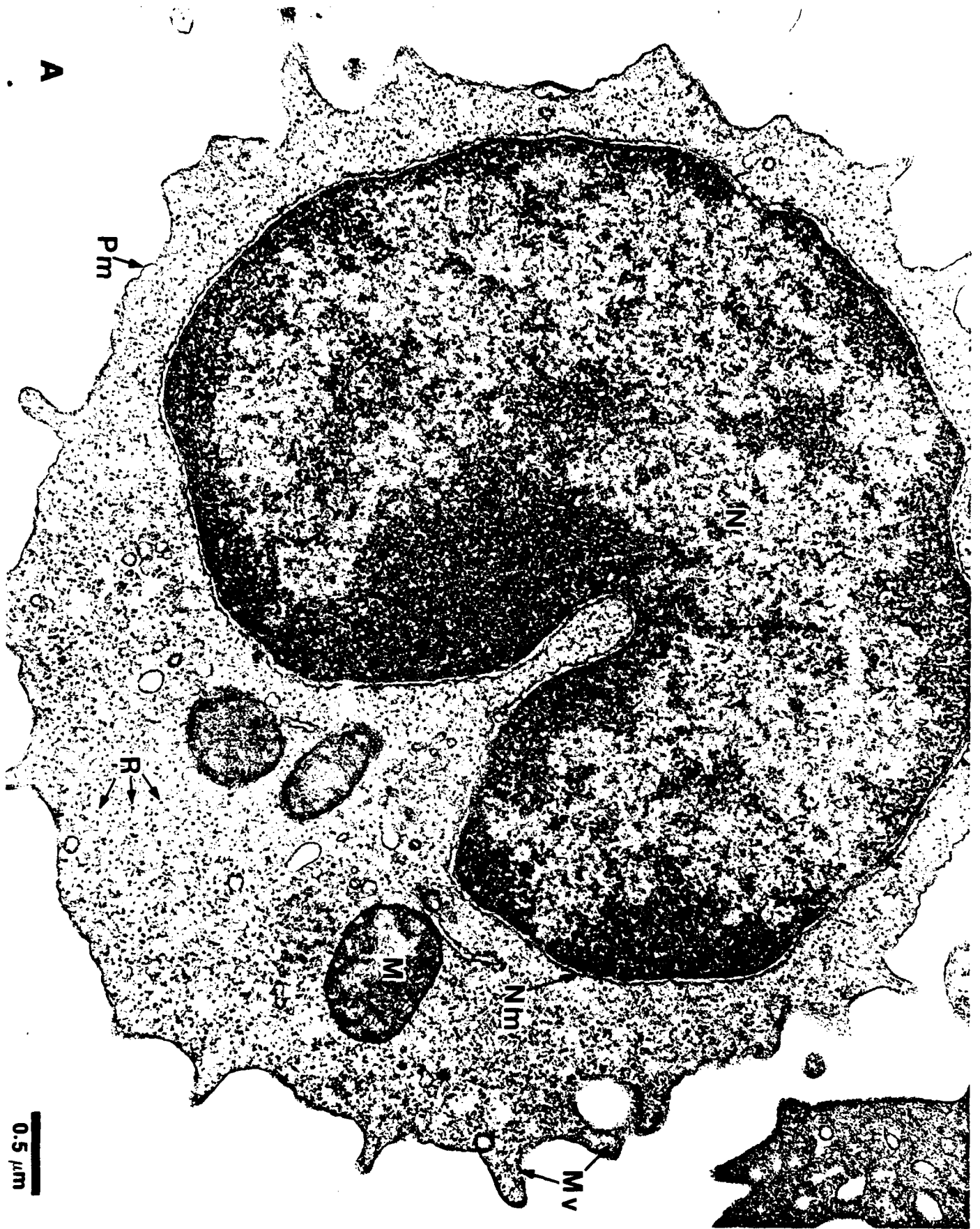
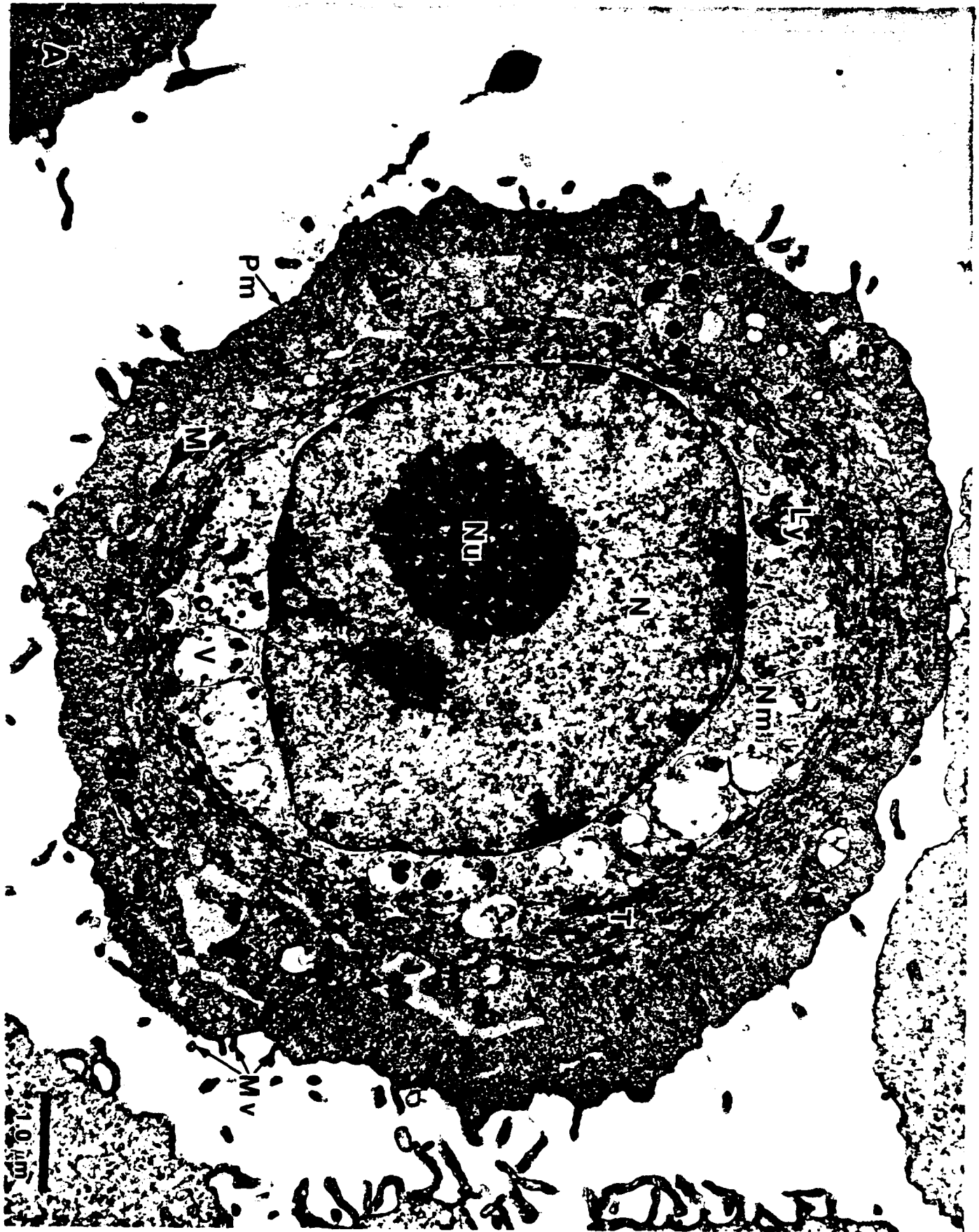
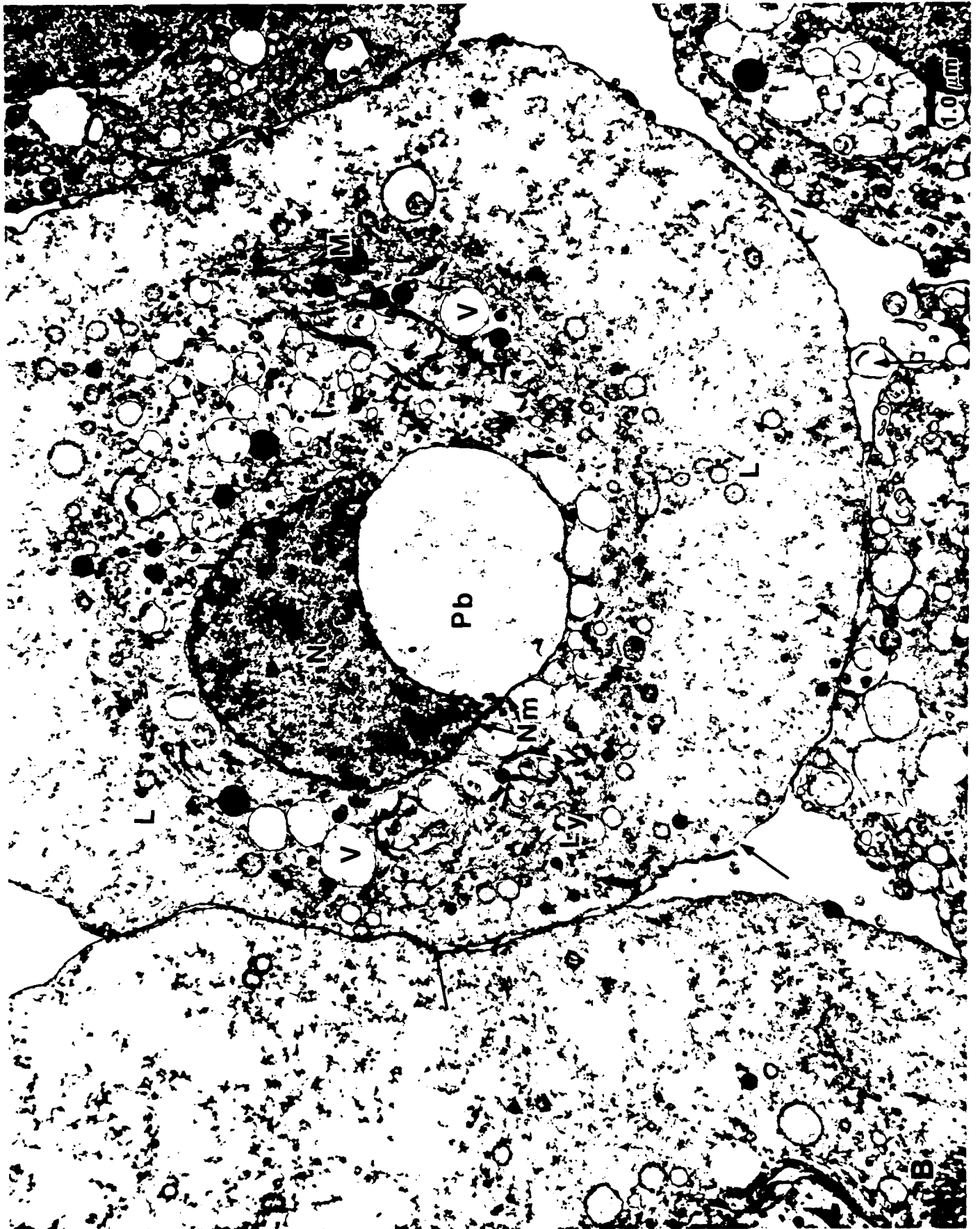


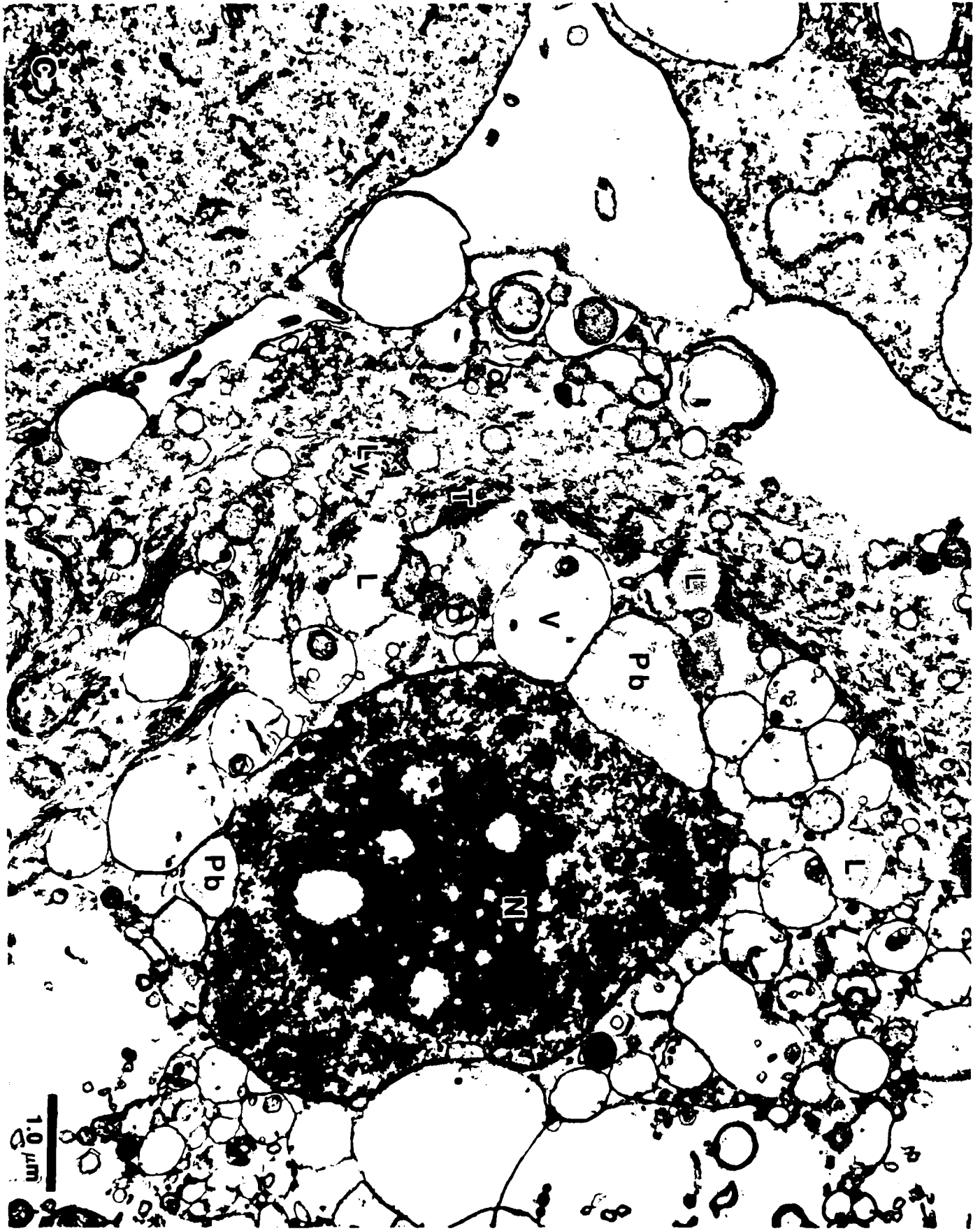




Figure 9. Transmission electron microscopy of human keratinocytes. A. Representative cell of the control group with ultrastructural features typical of a keratinocyte in culture; nucleus (N), nucleolus (Nu), nuclear membrane (Nm), mitochondria (M), lysosome (Ly), endocytotic vacuoles (V), tonofibrils (T), microvilli (Mv). B,C. Keratinocytes exposed to HD showing similar subcellular changes as seen in the exposed lymphocyte to include loss of microvilli, nuclear condensations, progressive cytoplasmic vacuolations, blebbing of the nuclear membrane (Pb), loss of tonofibrils, perforations of the plasmalemma (arrows), increased lysosomal (Ly) activity and lipid (L) deposition.







REFERENCES

1. Papirmeister, B.; Gross, C.L.; Petrali, J.P.; and Hixson, C.J.: Pathology Produced by Sulfur Mustard in Human Skin Grafts on Athymic Nude Mice. J. Toxicol. Cut. Ocular Toxicol. 3(4):371-408, 1984.
2. Meier, H.L.; Petrali, J.P.; and Gross, C.L.: Evidence that Niacinamide Prevents Sulfur Mustard (HD)-initiated Damage to Both Nucleus and Cytoplasmic Organelles of Human Lymphocytes Abstract (431). Faseb Journal 2, No. 4 1988, p.A373.
3. Petrali, J.P.; Oglesby, S.B.; and Meier H.L.: Ultrastructural Correlates of the Protection Afforded by Niacinamide Against Sulfur Mustard-induced Cytotoxicity of Human Lymphocytes In vitro. USAMRICD-TR-88-16, U.S. Army Medical Research Instit. of Chemical Defense, APG, MD, December 1988, AD# A203 118.
4. Marlow, D.D.; Mershon, M.M.; Mitcheltree, L.W.; Petrali, J.P.; Jaax, G.P.: Evaluation of Euthymic Hairless Guinea Pigs [CrI:IAF(HA)BR] as an Animal Model for Vesicant Injury. USAMRICD-TR-89-02, U.S. Army Medical Research Instit. of Chemical Defense, APG, MD, May 1989, AD# A209 293.
5. Humphrey, C.D. and Pittman, F.E.: A Simple Methylene Blue, Azure II, and Basic Fuchsin Stain for Epoxy Embedded Tissue Sections. Stain Technology, Vol. 49, No 9, 1974.
6. Kahl, F.R. and Pearson, R.W.: Ultrastructural Studies of Experimental Vesiculation. II. Collagenase. J. Invest. Derm. 49, No. 6, 1967.
7. Einbinder, J.M.; Walzer, R.A.; and Mandl, I.: Epidermal-dermal Separation with Proteolytic Enzymes. J. Invest. Derm. 46, No. 5, 1966.

Distribution List

Addresses	Copies	Addresses	Copies
Defense Technical Information Center ATTN: DTIC-DDAC Cameron Station, Bldg 5 Alexandria, VA 22304-6145	12	Commander US Army Research Institute of Environmental Medicine Bldg 42 Natick, MA 01760-5007	1
Commander US Army Medical Research and Development Command Fort Detrick, MD 21701-5012	2	Commandant US Army Chemical School ATTN: ATZN-CM-C Fort McClellan, AL 36205	1
HQDA (DASG-HCD) Washington, DC 20310	1	Director Armed Forces Medical Intelligence Center Fort Detrick, MD 21701-5004	1
Director Walter Reed Army Institute of Research Bldg 40 Washington, DC 20307-5100	1	Commander US Army Institute of Dental Research Bldg 40 Washington, DC 20307-5100	1
Commander Letterman Army Institute of Research Bldg 1110 Presidio of San Francisco, CA 94129-6800	1	Commander US Army Institute of Surgical Research Bldg 2653 Fort Sam Houston, TX 78234-6200	1
Commander US Army Aeromedical Research Laboratory ATTN: Scientific Information Ctr P.O. Box 577 Fort Rucker, AL 36362-5000	1	Commandant Academy of Health Sciences US Army ATTN: HSHA-CDC Fort Sam Houston, TX 78234-6100	1
Commander US Army Biomedical Research and Development Laboratory Bldg 568 Fort Detrick, MD 21701-5010	1	Commandant Academy of Health Sciences US Army ATTN: HSHA-CDM Fort Sam Houston, TX 78234-6100	1
Commander US Army Medical Research Institute of Infectious Disease Bldg 1425 Fort Detrick, MD 21701-5011	1	Mr Thomas R. Dashiell Director, Environmental and Life Sciences Office of the Deputy Under Secretary of Defense (Rsch & Adv Technology) Room 3D129 Washington, DC 20301-2300	1

Commander US Army Training and Doctrine Command ATTN: ATMD Fort Monroe, VA 23651	1	Department of Health and Human Services National Institutes of Health The National Library of Medicine Serial Records Section 8600 Rockville Pike Bethesda, MD 20894	1
Commander US Army Nuclear and Chemical Agency 7500 Backlick Road Bldg 2073 Springfield, VA 22150-3198	1	Stemson Library Academy of Health Sciences Bldg 2840, Rm 106 Fort Sam Houston, TX 78234-6100	1
Biological Science Division Office of Naval Research Arlington, VA 22217	1	US Army Research Office ATTN: Chemical and Biological Sciences Division P.O. Box 12211 Research Triangle Park, NC 27709-2211	1
Executive Officer Naval Medical Research Institute Naval Medicine Command National Capital Region Bethesda, MD 20814	1	AFOSR/NL Bldg 410, Rm A217 Bolling AFB, DC 20332	1
USAF School of Aerospace Medicine/VN Crew Technology Division Brooks AFB, TX 78235-5000	1	Commander US Army Chemical Research, Development & Engineering Ctr ATTN: SMCCR-MIS Aberdeen Proving Ground, MD 21010-5423	1
Commander US Army Medical Research Institute of Chemical Defense ATTN: SGRD-UV-ZA SGRD-UV-ZB SGRD-UV-ZS (2 copies) SGRD-UV-RC (5 copies) SGRD-UV-R (13 copies) SGRD-UV-AI SGRD-UV-D SGRD-UV-P SGRD-UV-V SGRD-UV-Y Aberdeen Proving Ground, MD 21010-5425	27		